Weierstraß-Institut
für Angewandte Analysis und Stochastik

im Forschungsverbund Berlin e.V.

Preprint ISSN 0946 – 8633

Solving conical diffraction with integral equations

Leonid I. Goray [1], Gunther Schmidt[2]

submitted: December 7, 2009

[1] St. Petersburg Physics
and Technology Center
for Research and Education, RAS
Khlopina 8/3
St. Petersburg 194021
Russia

[2] Weierstrass Institute
for Applied Analysis and Stochastics
Mohrenstr. 39
10117 Berlin
Germany
E-Mail: schmidt@wias-berlin.de

No. 1469
Berlin 2009

2000 *Mathematics Subject Classification.* 78A45, 78M15, 65N38, 35J05, 35Q60, 45F15.

Key words and phrases. Diffraction, periodic structure, integral equation method, oblique incidence, energy conservation, numerical tests.

Edited by
Weierstraß-Institut für Angewandte Analysis und Stochastik (WIAS)
Mohrenstraße 39
10117 Berlin
Germany

Fax: + 49 30 2044975
E-Mail: preprint@wias-berlin.de
World Wide Web: http://www.wias-berlin.de/

Abstract. Off-plane scattering of time-harmonic plane waves by a diffraction grating with arbitrary conductivity and general border profile is considered in a rigorous electromagnetic formulation. The integral equations for conical diffraction were obtained using the boundary integrals of the single and double layer potentials including the tangential derivative of single layer potentials interpreted as singular integrals. We derive an important formula for the calculation of the absorption in conical diffraction. Some rules which are expedient for the numerical implementation of the theory are presented. The efficiencies and polarization angles compared with those obtained by Lifeng Li for transmission and reflection gratings are in a good agreement. The code developed and tested is found to be accurate and efficient for solving off-plane diffraction problems including high-conductive surfaces, borders with edges, real border profiles, and gratings working at short wavelengths.

1. Introduction

Today a lot of optical applications of conical diffraction (off-plane) by gratings are well known, in particular: gratings working in the x-ray and extreme ultraviolet (EUV) ranges at grazing angles; shallow and deep high-conductive, anomalously absorbing gratings illuminated at near normal and grazing incidence; high-spatial-frequency, deep transmission gratings having high anti-reflection and polarization conversion properties; generalized spectroscopic ellipsometry and scatterometry techniques. For the numerical simulation of conical diffraction by optical gratings of arbitrary groove profiles and conductivity several rigorous methods have been proposed. Among them we know: differential [1, 2], coordinate transformation [3, 4, 5, 6], modal [7], fictitious sources [8, 9], and finite element [10, 11] methods. In Ref. [12] T-matrix and integral equation methods were described for off-plane transmission and low-conducting sine-profiled gratings.

For the classical (in-plane) diffraction problems integral equation methods have been established as an efficient and accurate numerical tool. Many different, quite sophisticated integral formulations have been proposed and implemented, cf. e.g. [13, 14, 15, 16, 17, 18, 19, 20, 21, 22]. The methods are used to tackle successfully high-conductive deep-groove gratings in the TM polarization, profile curves with corners, echelles, gratings with thin coated layers, randomly rough mirrors and gratings, and diffraction problems at very small wavelength-to-period ratios [23, 24, 25, 26, 27, 28, 29, 30]. The aim of this paper is to study an integral method for conical diffraction on the simplest model, the diffraction of a time-harmonic plane wave by a surface, which in Cartesian coordinates (x, y, z) is periodic in x- and invariant in z-direction and separates two different materials. Special attention is paid to the main aspects of the integral equation method for arbitrarily polarized plane waves and gratings with one border having any outline and conductivity.

The electromagnetic formulation of the diffraction by general gratings, which are modeled as infinite periodic structures, can be reduced to a system of Helmholtz equations for the z-components of the electric and magnetic fields in $\mathbb{R}^2$, where the solutions have to be quasiperiodic in one variable, subject to radiation conditions with respect to the other and satisfy certain jump conditions at the interface between different materials of the diffraction grating. In the case of classical diffraction, when the incident wave vector is orthogonal to the z-direction, the system degenerates to independent transmission problems for the two basic polarizations of the incident wave, whereas for the case of conical diffraction the boundary values of the z-components as well as their normal and tangential derivatives at the interface are coupled. Thus the unknowns are scalar functions in the case of classical diffraction and they are two-component vector functions in the conical case.

In the case of one border we reduce the system of Helmholtz equations to a 2×2 system of integral equations, which contain, besides the boundary integrals of the single and double layer potentials, also the tangential derivative of single layer potentials which are singular integrals. The corresponding theory is described in Section 2. The diffraction problem and boundary relations between values of the fields across the boundary are formulated in the explicit form in Subsection 2.1 The respective integral equations in terms of boundary potentials with detailed discussions, formulas, and jump relations can be found in Subsection 2.2 A more general treatment of the energy conservation law applicable to off-plane absorption gratings is considered in Subsection 2.3. The numerical implementation approach expedient for the calculation of far-fields and polarization properties of conical diffraction by gratings is described briefly in Section 3. Diverse numerical tests devoted to comparing, convergence, accuracy, computation time, and obtaining results for an important case are given in Section 4. In Subsection 4.1 we compare some of our results with data obtained by other well-established conical approaches for different groove profile and conductivity gratings. Some information about convergence, accuracy, and complexity of the presented method is included in Subsection 4.2. Finally, in Subection 4.3 a numerical experiment for the off-plane grazing-incident real-groove-profile grating working in the soft x-ray range is demonstrated as an illustration of possibilities of the software developed.

2. Theory

2.1. **Diffraction problem.** We denote by $\mathbf{e}_x$, $\mathbf{e}_z$ and $\mathbf{e}_z$ the unit vectors of the axes of the Cartesian coordinates. The grating is a cylindrical surface whose generatrices are parallel to the z-axis and whose cross section is described by the curve Σ (see Fig. 1). We suppose that Σ is not self-intersecting and d-periodic in x-direction. The grating surface is the boundary between two regions $G_\pm \times \mathbb{R} \subset \mathbb{R}^3$ which are filled with materials of constant electric permittivity $\varepsilon_\pm$ and magnetic permeability $\mu_\pm$.

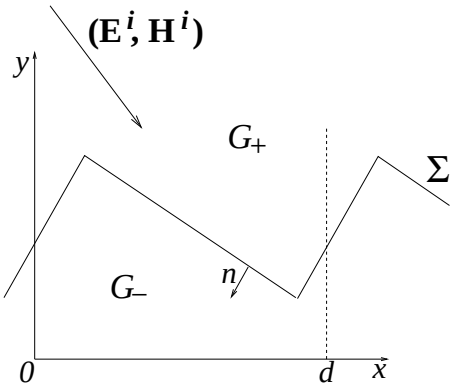

Figure 1. Schematic cross section of a simple grating

We deal only with time-harmonic fields; consequently, the electric and magnetic fields are represented by the complex vectors $\mathbf{E}$ and $\mathbf{H}$, with a time dependence $\exp(-i\omega t)$ taken into account. The wave vector $\mathbf{k}_+$ of the incident wave in $G_+ \times \mathbb{R}$, where $\varepsilon_+, \mu_+ > 0$, is in general not perpendicular to the grooves ($\mathbf{k}_+ \cdot \mathbf{e}_z \neq 0$). Setting $\mathbf{k}_+ = (\alpha, -\beta, \gamma)$ the surface is illuminated by a electromagnetic plane wave

$$\mathbf{E}^i = \mathbf{p}\, \mathrm{e}^{i(\alpha x - \beta y + \gamma z)}\,, \quad \mathbf{H}^i = \mathbf{s}\, \mathrm{e}^{i(\alpha x - \beta y + \gamma z)}\,,$$

which due to the periodicity of Σ is scattered into a finite number of plane waves in $G_+ \times \mathbb{R}$ and possibly in $G_- \times \mathbb{R}$. The wave vectors of these outgoing modes lie on the surface of a cone whose axis is parallel to the z–axis. Therefore one speaks of conical diffraction.

The components of $\mathbf{k}_+$ satisfy

$$\beta > 0 \quad \text{and} \quad \alpha^2 + \beta^2 + \gamma^2 = \omega^2 \varepsilon_+ \mu_+ \,,$$

and they are expressed using the incidence angles $|\theta|, |\phi| < \pi/2$

$$(\alpha, -\beta, \gamma) = \omega \sqrt{\varepsilon_+ \mu_+}\, (\sin\theta \cos\phi, -\cos\theta \cos\phi, \sin\phi)\,.$$

Classical diffraction corresponds to $\mathbf{k}_+ \cdot \mathbf{e}_z = 0$, whereas $\phi \neq 0$ characterizes conical diffraction.

Since the geometry is invariant with respect to any translation parallel to the z-axis, we make the ansatz for the total field

$$(\mathbf{E}, \mathbf{H})(x, y, z) = (E, H)(x, y)\, \mathrm{e}^{i\gamma z} \tag{1}$$

with $E, H : \mathbb{R}^2 \to \mathbb{C}^3$. This transforms the time-harmonic Maxwell equations in $\mathbb{R}^3$

$$\boldsymbol{\nabla} \times \mathbf{E} = i\omega\mu \mathbf{H} \quad \text{and} \quad \boldsymbol{\nabla} \times \mathbf{H} = -i\omega\varepsilon \mathbf{E}\,, \tag{2}$$

with piecewise constant functions $\varepsilon(x, y) = \varepsilon_\pm$, $\mu(x, y) = \mu_\pm$ for $(x, y) \in G_\pm$, into a two-dimensional problem. This was described in [9] and analytically justified in [31]. Introducing the transverse components

$$E_T = E - E_z \mathbf{e}_z\,, \quad H_T = H - H_z \mathbf{e}_z\,,$$

representation (1) and equations (2) lead to

$$\nabla E_z = i\gamma E_T + i\omega\mu\, \mathbf{e}_z \times H_T\,, \quad \nabla H_z = i\gamma H_T - i\omega\varepsilon\, \mathbf{e}_z \times E_T\,.$$

This shows that the field has locally a finite energy, i.e.

$$\mathbf{E}\,,\ \mathbf{H}\,,\ \boldsymbol{\nabla} \times \mathbf{E}\,,\ \boldsymbol{\nabla} \times \mathbf{H} \in \big(L^2_{loc}(\mathbb{R}^3)\big)^3\,,$$

if and only if the z-components of E, H satisfy $\nabla E_z, \nabla H_z \in L^2_{loc}(\mathbb{R}^2)$. Moreover, from Maxwell's equations (2) one gets

$$(\omega^2\varepsilon\mu - \gamma^2) E_T = i\gamma \nabla E_z + i\omega\mu \nabla \times H_z\,, \quad (\omega^2\varepsilon\mu - \gamma^2) H_T = i\gamma \nabla H_z - i\omega\varepsilon \nabla \times E_z\,. \tag{3}$$

Noting $\gamma = \omega(\varepsilon_+\mu_+)^{1/2} \sin\phi$, we introduce the piecewise constant function

$$\kappa(x, y) = \begin{cases} (\varepsilon_+\mu_+ - \varepsilon_+\mu_+ \sin^2\phi)^{1/2} = \kappa_+\,, & (x, y) \in G_+\,, \\ (\varepsilon_-\mu_- - \varepsilon_+\mu_+ \sin^2\phi)^{1/2} = \kappa_-\,, & (x, y) \in G_-\,, \end{cases} \tag{4}$$

with the square root $z^{1/2} = r^{1/2} \exp(i\varphi/2)$ for $z = r \exp(i\varphi)$, $0 \leq \varphi < 2\pi$. Hence (3) shows that under the condition $\kappa \neq 0$, which will be assumed throughout, the components E_z, H_z determine the electromagnetic field $(\mathbf{E}, \mathbf{H})$.

The equations (2) imply that E_z, H_z satisfy the Helmholtz equations

$$(\Delta + \omega^2\kappa^2)\, E_z \,= (\Delta + \omega^2\kappa^2)\, H_z \,= 0 \tag{5}$$

in $G_\pm$. The continuity of the tangential components of $\mathbf{E}$ and $\mathbf{H}$ on the surface takes the form

$$\big[(n, 0) \times E\big]_{\Sigma\times\mathbb{R}} = \big[(n, 0) \times H\big]_{\Sigma\times\mathbb{R}} = 0\,,$$

where $(n, 0) = (n_x, n_y, 0)$ is the normal vector on $\Sigma \times \mathbb{R}$ and $\big[(n, 0) \times E\big]_{\Sigma\times\mathbb{R}}$ denotes the jump of the function $(n, 0) \times E$ across the surface. This leads to the jump conditions

$$\big[E_z\big]_\Sigma = \big[H_z\big]_\Sigma = 0\,, \ \Big[\frac{\gamma}{\omega^2\kappa^2}\, \partial_t H_z + \frac{\omega\varepsilon}{\omega^2\kappa^2}\, \partial_n E_z\Big]_\Sigma = \Big[\frac{\gamma}{\omega^2\kappa^2}\, \partial_t E_z - \frac{\omega\mu}{\omega^2\kappa^2}\, \partial_n H_z\Big]_\Sigma = 0\,.$$

Here $\partial_n = n_x\partial_x + n_y\partial_y$ and $\partial_t = -n_y\partial_x + n_x\partial_y$ are the normal and tangential derivatives on Σ, respectively. We introduce $B_z = (\mu_+/\varepsilon_+)^{1/2} H_z$ and use $\gamma = \omega(\varepsilon_+\mu_+)^{1/2}\sin\phi$ to rewrite the jump conditions in the form

$$[E_z]_\Sigma = [H_z]_\Sigma = 0\,,\ \Big[\frac{\varepsilon\,\partial_n E_z}{\kappa^2}\Big]_\Sigma = -\varepsilon_+\sin\phi\Big[\frac{\partial_t B_z}{\kappa^2}\Big]_\Sigma,\ \Big[\frac{\mu\,\partial_n B_z}{\kappa^2}\Big]_\Sigma = \mu_+\sin\phi\Big[\frac{\partial_t E_z}{\kappa^2}\Big]_\Sigma. \tag{6}$$

The z-components of the incoming field

$$E_z^i(x,y) = p_z\,\mathrm{e}^{i(\alpha x-\beta y)}\,,\ B_z^i(x,y) = q_z\,\mathrm{e}^{i(\alpha x-\beta y)}\,, \tag{7}$$

are α-quasiperiodic in x of period d, i.e. satisfy the relation

$$u(x+d,y) = \mathrm{e}^{id\alpha}\,u(x,y)\,.$$

In view of the periodicity of ε and μ this motivates to seek α-quasiperiodic solutions E_z, B_z. Furthermore, the diffracted fields must remain bounded at infinity, which implies the well known outgoing wave condition

$$\begin{aligned}(E_z,B_z)(x,y) &= (E_z^i,B_z^i) + \sum_{n\in\mathbb{Z}}(E_n^+,B_n^+)\,\mathrm{e}^{i(\alpha_n x+\beta_n^+ y)}, && y\ge H,\\ (E_z,B_z)(x,y) &= \sum_{n\in\mathbb{Z}}(E_n^-,B_n^-)\,\mathrm{e}^{i(\alpha_n x-\beta_n^- y)}, && y\le -H,\end{aligned} \tag{8}$$

where $\Sigma\subset\{(x,y):|y|<H\}$, and α_n, $\beta_n^\pm$ are given by

$$\alpha_n = \alpha + \frac{2\pi n}{d}\,,\quad \beta_n^\pm = \sqrt{\omega^2\kappa_\pm^2-\alpha_n^2}\quad\text{with } 0\le\arg\beta_n^\pm<\pi\,.$$

In the following it is always assumed that

$$0\le\arg\varepsilon_-,\arg\mu_-\le\pi\quad\text{with}\quad\arg(\varepsilon_-\mu_-)<2\pi\,, \tag{9}$$

which holds for all existing optical (meta)materials. Then $0\le\arg\kappa_-^2<2\pi$ and β_n^- are properly defined for all n.

Denoting the z-components of the total fields

$$E_z = \begin{cases} u_+ + E_z^i \\ u_- \end{cases},\quad B_z = \begin{cases} v_+ + B_z^i & \text{in } G_+,\\ v_- & \text{in } G_-\,,\end{cases}$$

the problem (5), (6), (8) can be written as

$$\Delta u_\pm + \omega^2\kappa_\pm^2 u_\pm = \Delta v_\pm + \omega^2\kappa_\pm^2 v_\pm = 0\quad\text{in } G_\pm, \tag{10}$$

$$\left.\begin{aligned} &u_- = u_+ + E_z^i,\ \ \frac{\varepsilon_-\,\partial_n u_-}{\kappa_-^2} - \frac{\varepsilon_+\partial_n(u_+ + E_z^i)}{\kappa_+^2} = \varepsilon_+\sin\phi\,\Big(\frac{1}{\kappa_+^2}-\frac{1}{\kappa_-^2}\Big)\partial_t v_-,\\ &v_- = v_+ + B_z^i,\ \ \frac{\mu_-\partial_n v_-}{\kappa_-^2} - \frac{\mu_+\partial_n(v_+ + B_z^i)}{\kappa_+^2} = -\mu_+\sin\phi\,\Big(\frac{1}{\kappa_+^2}-\frac{1}{\kappa_-^2}\Big)\partial_t u_-,\end{aligned}\right\}\quad\text{on } \Sigma \tag{11}$$

$$\begin{aligned}(u_+,v_+)(x,y) &= \sum_{n=-\infty}^{\infty}(E_n^+,B_n^+)\,\mathrm{e}^{i(\alpha_n x+\beta_n^+ y)} && \text{for } y\ge H,\\ (u_-,v_-)(x,y) &= \sum_{n=-\infty}^{\infty}(E_n^-,B_n^-)\,\mathrm{e}^{i(\alpha_n x-\beta_n^- y)} && \text{for } y\le -H.\end{aligned} \tag{12}$$

2.2. **Integral equations.** There exist different ways to transform the transmission problem for the Helmholtz equations in $\mathbb{R}^2$ (10) - (12) to integral equations. We combine here the direct and indirect approach as proposed in [23, 24] for the case of classical diffraction. Let Σ be given by a piecewise C^2 parametrization

$$\sigma(t) = (X(t), Y(t)), \quad X(t+1) = X(t) + d,\ Y(t+1) = Y(t)\,, \quad t \in \mathbb{R}\,, \tag{13}$$

i.e. the continuous functions X, Y are piecewise C^2 and $\sigma(t_1) \neq \sigma(t_2)$ if $t_1 \neq t_2$. If the profile Σ has corners, then we suppose additionally that the angles between adjacent tangents at the corners are strictly between 0 and 2π.

The potentials which provide α-quasiperiodic solutions of the Helmholtz equation

$$\Delta u + k^2 u = 0 \qquad \text{with } 0 \leq \arg k^2 < 2\pi \tag{14}$$

are based on the quasiperiodic fundamental solution of period d

$$\Psi_{k,\alpha}(P) = \lim_{N\to\infty} \frac{i}{2d} \sum_{n=-N}^{N} \frac{\mathrm{e}^{\,i\alpha_n X + i\beta_n |Y|}}{\beta_n}\,, \quad P = (X, Y)\,.$$

Here we assume that $\beta_n = (k^2 - \alpha_n^2)^{1/2} \neq 0$ for all n. The single and double layer potentials are defined by

$$\begin{aligned} \mathcal{S}_{k,\alpha}\varphi(P) &= 2\int_\Gamma \varphi(Q)\, \Psi_{k,\alpha}(P-Q)\, d\sigma_Q\,, \\ \mathcal{D}_{k,\alpha}\varphi(P) &= 2\int_\Gamma \varphi(Q)\, \partial_{n(Q)} \Psi_{k,\alpha}(P-Q)\, d\sigma_Q\,, \end{aligned} \tag{15}$$

where Γ is one period of the interface Σ, i.e. $\Gamma = \{\sigma(t) : t \in [t_0, t_0+1]\}$ for some t_0. In (15) $d\sigma_Q$ denotes the integration with respect to the arc length and $n(Q)$ is the normal to Σ at $Q \in \Sigma$ pointing into G_-. Obviously, for α-quasiperiodic densities φ on Σ the value of the potentials does not depend on the choice of Γ.

The potentials provide the usual representation formulas. Any α-quasiperiodic function u which satisfies in G_+ the Helmholtz equation (14) and the radiation condition

$$u(x,y) = \sum_{n=-\infty}^{\infty} u_n\, \mathrm{e}^{\,i\alpha_n x + i\beta_n |y|}\,, \quad |y| \geq H\,.$$

admits the representation

$$\frac{1}{2}\big(\mathcal{S}_{k,\alpha}\partial_n u - \mathcal{D}_{k,\alpha} u\big) = \begin{cases} u & \text{in } G_+, \\ 0 & \text{in } G_-, \end{cases} \tag{16}$$

where the normal n points into G_-. Under the same assumptions for a function u in G_- the representation

$$\frac{1}{2}\big(\mathcal{D}_{k,\alpha} u - \mathcal{S}_{k,\alpha}\partial_n u\big) = \begin{cases} 0 & \text{in } G_+, \\ u & \text{in } G_-, \end{cases} \tag{17}$$

is valid.

Restriction of the potentials $\mathcal{S}_{k,\alpha}$ and $\mathcal{D}_{k,\alpha}$ to the profile curve Σ are the so called boundary integral operators. The potentials provide the usual jump relations of classical potential theory. The single layer potential is continuous across Σ

$$(\mathcal{S}_{k,\alpha}\varphi)^+(P) = (\mathcal{S}_{k,\alpha}\varphi)^-(P) = V_{k,\alpha}\varphi(P)\,,$$

where the upper sign + resp. − denotes the limits of the potentials for points in $G_\pm$ tending in non-tangential direction to $P \in \Sigma$, and $V_{k,\alpha}$ is a integral operator with logarithmic singularity

$$V_{k,\alpha}\varphi(P) = 2\int_\Gamma \Psi_{k,\alpha}(P-Q)\,\varphi(Q)\,d\sigma_Q\,, \quad P \in \Sigma\,.$$

The double layer potential has a jump if crossing Γ:

$$\big(\mathcal{D}_{k,\alpha}\varphi\big)^+ = (K_{k,\alpha} - I)\varphi, \quad \big(\mathcal{D}_{k,\alpha}\varphi\big)^- = (K_{k,\alpha} + I)\varphi \tag{18}$$

with the boundary double layer potential

$$K_{k,\alpha}\varphi(P) = 2\int_\Gamma \varphi(Q)\,\partial_{n(Q)}\Psi_{k,\alpha}(P-Q)\,d\sigma_Q + (\delta(P)-1)\varphi(P)\,.$$

Here $\delta(P) \in (0,2)$, $P \in \Sigma$, denotes the ratio of the angle in G_+ at P and π, i.e. $\delta(P) = 1$ outside corner points of Σ. The normal derivative of $\mathcal{S}_{k,\alpha}\varphi$ at Σ exists outside corners and has the limits

$$\big(\partial_n\mathcal{S}_{k,\alpha}\varphi\big)^+ = (L_{k,\alpha} + I)\varphi, \quad \big(\partial_n\mathcal{S}_{k,\alpha}\varphi\big)^- = (L_{k,\alpha} - I)\varphi, \tag{19}$$

where $L_{k,\alpha}$ is the integral operator on Γ with the kernel $\partial_{n(P)}\Psi_{k,\alpha}(P-Q)$,

$$L_{k,\alpha}\varphi(P) = 2\int_\Gamma \varphi(Q)\,\partial_{n(P)}\Psi_{k,\alpha}(P-Q)\,d\sigma_Q\,, \quad P \in \Sigma\,.$$

In the following also the tangential derivative of single layer potentials

$$\partial_t\big(V_{k,\alpha}\varphi\big)(P) = 2\,\partial_t\int_\Gamma \Psi_{k,\alpha}(P-Q)\,\varphi(Q)\,d\sigma_Q\,, \quad P \in \Sigma\,,$$

occurs. Interchanging differentiation and integration leads to a kernel with the main singularity

$$\frac{t(P)\cdot(P-Q)}{|P-Q|^2}\,,$$

therefore the tangential derivative of single layer potentials cannot be expressed as usual integral. But it can be interpreted as Cauchy principal value or singular integral

$$J_{k,\alpha}\varphi(P) = 2\lim_{\delta\to 0}\int_{\Gamma\setminus\Gamma(P,\delta)} \varphi(Q)\,\partial_{t(P)}\Psi_{k,\alpha}(P-Q)\,d\sigma_Q = \partial_t\big(V_{k,\alpha}\varphi\big)(P)\,, \tag{20}$$

where $\Gamma(P,\delta)$ is the subarc of Γ of length 2δ with the mid point P. Similarly, one can define the singular integral

$$H_{k,\alpha}\varphi(P) = 2\lim_{\delta\to 0}\int_{\Gamma\setminus\Gamma(P,\delta)} \varphi(Q)\,\partial_{t(Q)}\Psi_{k,\alpha}(P-Q)\,d\sigma_Q\,, \tag{21}$$

which by using integration by parts gives for α-quasiperiodic φ

$$H_{k,\alpha}\varphi(P) = -2\int_\Gamma \Psi_{k,\alpha}(P-Q)\,\partial_t\varphi(Q)\,d\sigma_Q = -V_{k,\alpha}\big(\partial_t\varphi\big)(P)\,, \quad P \in \Sigma\,.$$

Note that $V_{k,\alpha}\partial_t V_{k,\alpha} = V_{k,\alpha}J_{k,\alpha} = -H_{k,\alpha}V_{k,\alpha}$.

Now we are in the position to formulate the integral equations for solving the conical diffraction problem (10) – (12). In order to represent $u_\pm$ and $v_\pm$ as layer potentials we assume in what follows that the parameters are such that $\beta_n^\pm = (\omega^2\kappa_\pm^2 - \alpha_n^2)^{1/2} \neq 0$ for all n. Since

$\arg\kappa_- \in [0,\pi)$ (see assumption (9)) the boundary integral operators corresponding to the fundamental solution $\Psi_{\omega\kappa_\pm,\alpha}$ are well defined and by the representation formulas (16), (17)

$$u_+ = \frac{1}{2}\big(\mathcal{S}_\alpha^+\partial_n u_+ - \mathcal{D}_\alpha^+ u_+\big), \qquad v_+ = \frac{1}{2}\big(\mathcal{S}_\alpha^+\partial_n v_+ - \mathcal{D}_\alpha^+ v_+\big) \qquad \text{in } G_+\,,$$
$$E_z^i = \frac{1}{2}\big(\mathcal{D}_\alpha^+ E_z^i - \mathcal{S}_\alpha^+\partial_n E_z^i\big), \qquad B_z^i = \frac{1}{2}\big(\mathcal{D}_\alpha^+ B_z^i - \mathcal{S}_\alpha^+\partial_n B_z^i\big) \qquad \text{in } G_-\,.$$

Here we denote by $\mathcal{S}_\alpha^\pm$ the single layer potential defined on Γ with the fundamental solution $\Psi_{\omega\kappa_\pm,\alpha}$. Correspondingly $\mathcal{D}_\alpha^\pm$ is the double layer potential over Γ with the normal derivative of $\Psi_{\omega\kappa_\pm,\alpha}$ as kernel function. Taking the limits on Σ the jump relations (18) lead to

$$\begin{aligned} &V_\alpha^+\partial_n(u_+ + E_z^i) - \big(I + K_\alpha^+\big)\,(u_+ + E_z^i) = 2E_z^i|_\Sigma\,,\\ &V_\alpha^+\partial_n(v_+ + B_z^i) - \big(I + K_\alpha^+\big)\,(v_+ + B_z^i) = 2B_z^i|_\Sigma\,, \end{aligned} \tag{22}$$

where $V_\alpha^\pm$ denote the boundary single layer potentials

$$V_\alpha^\pm\varphi(P) = 2\int_\Gamma \varphi(Q)\,\Psi_{\omega\kappa_\pm,\alpha}(P-Q)\,d\sigma_Q\,, \quad P\in\Sigma\,,$$

and the operators $K_\alpha^\pm$ and $L_\alpha^\pm$ are defined analogously. The solutions in G_- are sought as single layer potentials

$$u_- = \mathcal{S}_\alpha^- w\,, \quad v_- = \mathcal{S}_\alpha^-\tau$$

with certain auxiliary densities w,τ. Since by Eq. (19)

$$u_-|_\Sigma = V_\alpha^- w,\ \partial_n u_-|_\Sigma = (L_\alpha^- - I)w,\ v_-|_\Sigma = V_\alpha^-\tau,\ \partial_n v_-|_\Sigma = (L_\alpha^- - I)\tau,$$

we see from the equations (22) that the jump conditions (11) are valid, when the unknowns w,τ satisfy the system of integral equations

$$\begin{aligned} &\frac{\varepsilon_-\kappa_+^2}{\varepsilon_+\kappa_-^2}V_\alpha^+(L_\alpha^- - I)w - \big(I + K_\alpha^+\big)\,V_\alpha^- w - \sin\phi\Big(1 - \frac{\kappa_+^2}{\kappa_-^2}\Big)V_\alpha^+\partial_t V_\alpha^-\tau = 2E_z^i,\\ &\frac{\mu_-\kappa_+^2}{\mu_+\kappa_-^2}V_\alpha^+(L_\alpha^- - I)\tau - \big(I + K_\alpha^+\big)\,V_\alpha^-\tau + \sin\phi\Big(1 - \frac{\kappa_+^2}{\kappa_-^2}\Big)V_\alpha^+\partial_t V_\alpha^- w = 2B_z^i. \end{aligned} \tag{23}$$

Recall that we suppose $\kappa_-^2 \neq 0$ and $\omega^2\kappa_\pm^2 - \alpha_n^2 \neq 0$ for all n.

For the analytical and numerical treatment of the integral equation system (23) it is advantageous to use the relations

$$V_\alpha^+\partial_t V_\alpha^- = -H_\alpha^+ V_\alpha^- = V_\alpha^+ J_\alpha^-$$

(see the definitions (20), (21)). Then (23) becomes a system of singular integral equations, for which exist powerful analytical and numerical methods.

If the solution of the system (23) is found, then the solution of the conical diffraction problem (10) - (12) can be determined by the relations

$$u_+ = -\frac{1}{2}\Big(\frac{\varepsilon_-\kappa_+^2}{\varepsilon_+\kappa_-^2}\,\mathcal{S}_\alpha^+(I - L_\alpha^-)w + \mathcal{D}_\alpha^+ V_\alpha^- w + \frac{\sin\phi(\kappa_-^2 - \kappa_+^2)}{\kappa_-^2}\,\mathcal{S}_\alpha^+ J_\alpha^-\tau\Big)\,, \quad u_- = \mathcal{S}_\alpha^- w\,,$$
$$v_+ = -\frac{1}{2}\Big(\frac{\mu_-\kappa_+^2}{\mu_+\kappa_-^2}\,\mathcal{S}_\alpha^+\,(I - L_\alpha^-)\tau + \mathcal{D}_\alpha^+ V_\alpha^-\tau - \frac{\sin\phi(\kappa_-^2 - \kappa_+^2)}{\kappa_-^2}\,\mathcal{S}_\alpha^+ J_\alpha^- w\Big)\,, \quad v_- = \mathcal{S}_\alpha^-\tau\,.$$

A detailed mathematical analysis of the system of singular integral equations (23) is given in [32]. In particular, the following properties have been established:

1. The integral equations are equivalent to the Helmholtz system if the operators V_α^+ and V_α^- are invertible.

2. If the profile Σ has no corners, then (23) is solvable if $\varepsilon_- + \varepsilon_+ \neq 0$ and $\mu_- + \mu_+ \neq 0$.
3. If the profile Σ has corners, then (23) is solvable if $\varepsilon_-/\varepsilon_+$ and $\mu_-/\mu_+ \notin [-\rho, -1/\rho]$ for some $\rho > 1$, depending on the angles at these corners.
4. The solution of (23) is unique if $\operatorname{Im}\varepsilon_- \geq 0$ and $\operatorname{Im}\mu_- \geq 0$ with $\operatorname{Im}(\varepsilon_- + \mu_-) > 0$

2.3. **Energy balance for conical diffraction.** Suppose that E_z, B_z are a solution of the partial differential formulation of conical diffraction (5), (6) and (8). The expression of the conservation of energy is based on a variational equality for E_z and B_z in a periodic cell Ω_H, which has in x-direction the width d, is bounded by the straight lines $\{y = \pm H\}$ and contains Γ. We multiply the Helmholtz equations (5) respectively with

$$\frac{\varepsilon}{\varepsilon_+\kappa^2}\,\overline{E_z} \quad \text{and} \quad \frac{\mu}{\mu_+\kappa^2}\,\overline{B_z}\,,$$

and apply Green's formula in the subdomains $\Omega_H \cap G_\pm$. Then by using the quasiperiodicity of E_z, B_z and the jump relations (6) one derives

$$\begin{aligned}\int_{\Omega_H} \frac{\varepsilon}{\varepsilon_+}\Big(\frac{1}{\kappa^2}|\nabla E_z|^2 - \omega^2\,|E_z|^2\Big) + \sin\phi\Big(\frac{1}{\kappa_+^2} - \frac{1}{\kappa_-^2}\Big)\int_\Gamma \partial_t B_z\,\overline{E_z}\\ - \frac{1}{\kappa_+^2}\int_{\Gamma(H)} \partial_n E_z\,\overline{E_z} - \frac{\varepsilon_-}{\varepsilon_+\kappa_-^2}\int_{\Gamma(-H)} \partial_n E_z\,\overline{E_z} = 0\,, \qquad (24)\end{aligned}$$

$$\begin{aligned}\int_{\Omega_H} \frac{\mu}{\mu_+}\Big(\frac{1}{\kappa^2}|\nabla B_z|^2 - \omega^2\,|B_z|^2\Big) - \sin\phi\Big(\frac{1}{\kappa_+^2} - \frac{1}{\kappa_-^2}\Big)\int_\Gamma \partial_t E_z\,\overline{B_z}\\ - \frac{1}{\kappa_+^2}\int_{\Gamma(H)} \partial_n B_z\,\overline{B_z} - \frac{\mu_-}{\mu_+\kappa_-^2}\int_{\Gamma(-H)} \partial_n B_z\,\overline{B_z} = 0\,, \qquad (25)\end{aligned}$$

where $\Gamma(\pm H)$ denotes the upper and lower straight boundary of Ω_H, respectively. The outgoing wave condition (7) and (8) implies

$$\int_{\Gamma(H)} \partial_n E_z\,\overline{E_z} = i\beta\Big(|E_0^+|^2 - |p_z|^2 + 2i\,\operatorname{Im}\big(E_0^+\overline{p_z}\,\mathrm{e}^{i\beta H}\big)\Big) + i\sum_{n\neq 0}\beta_n^+|E_n^+|^2\;\mathrm{e}^{-2H\operatorname{Im}\beta_n^+},$$

$$\int_{\Gamma(-H)} \partial_n E_z\,\overline{E_z} = i\sum_{n\in\mathbb{Z}}\beta_n^-|E_n^-|^2\;\mathrm{e}^{-2H\operatorname{Im}\beta_n^-},$$

and similar expressions for the boundary integrals involving B_z. Note that ε_+ and μ_+ are positive.

Let ε_- and μ_- be real. Taking the imaginary part of Eqs. (24) and (25) leads to the equations

$$\frac{\beta}{\kappa_+^2}|p_z|^2 - \frac{1}{\kappa_+^2}\sum_{\beta_n^+>0}\beta_n^+|E_n^+|^2 - \frac{\varepsilon_-}{\varepsilon_+\kappa_-^2}\sum_{\beta_n^->0}\beta_n^-|E_n^-|^2 = -\sin\phi\Big(\frac{1}{\kappa_+^2} - \frac{1}{\kappa_-^2}\Big)\operatorname{Im}\int_\Gamma \partial_t B_z\,\overline{E_z}\,,$$

$$\frac{\beta}{\kappa_+^2}|q_z|^2 - \frac{1}{\kappa_+^2}\sum_{\beta_n^+>0}\beta_n^+|B_n^+|^2 - \frac{\mu_-}{\mu_+\kappa_-^2}\sum_{\beta_n^->0}\beta_n^-|B_n^-|^2 = \sin\phi\Big(\frac{1}{\kappa_+^2} - \frac{1}{\kappa_-^2}\Big)\operatorname{Im}\int_\Gamma \partial_t E_z\,\overline{B_z}\,.$$

Since

$$\operatorname{Im}\int_\Gamma \partial_t B_z\,\overline{E_z} = \operatorname{Im}\int_\Gamma \partial_t E_z\,\overline{B_z}$$

we derive

$$|p_z|^2 + |q_z|^2 = \sum_{\beta_n^+>0}\frac{\beta_n^+}{\beta}\big(|E_n^+|^2 + |B_n^+|^2\big) + \frac{\kappa_+^2}{\kappa_-^2}\sum_{\beta_n^->0}\frac{\beta_n^-}{\beta}\Big(\frac{\varepsilon_-}{\varepsilon_+}|E_n^-|^2 + \frac{\mu_-}{\mu_+}|B_n^-|^2\Big)\,.$$

Thus for lossless gratings the energy of the incident wave $|p_z|^2 + |q_z|^2$ equals the sum of reflection order efficiencies

$$R = \sum_{\beta_n^+ > 0} \frac{\beta_n^+}{\beta} \big(|E_n^+|^2 + |B_n^+|^2 \big)$$

plus the sum of transmission order efficiencies

$$T = \sum_{\beta_n^- > 0} \frac{\beta_n^-}{\beta} \Big(\frac{\varepsilon_-}{\varepsilon_+} |E_n^-|^2 + \frac{\mu_-}{\mu_+} |B_n^-|^2 \Big) .$$

If $\operatorname{Im} \varepsilon_- \neq 0$ or $\operatorname{Im} \mu_- \neq 0$, then $T = 0$ and $|p_z|^2 + |q_z|^2 > R$, i.e. the usual conservation of energy does not hold. Instead, one part of the energy is absorbed in the substrate. This heat absorption energy plus the energy of the reflected modes equals the energy of the incident wave.

Therefore, one tool to check the quality of the numerical solution for absorbing gratings is the requirement, that the sum of the reflected energy and the absorption energy should be equal to the energy of the incident wave.

To obtain an expression for the absorption energy we note that by Green's formula

$$\begin{aligned}
\int_{\Omega_H \cap G_-} \frac{\varepsilon_-}{\varepsilon_+} \Big(\frac{1}{\kappa_-^2} |\nabla E_z|^2 - \omega^2 |E_z|^2 \Big) - \frac{\varepsilon_-}{\varepsilon_+ \kappa_-^2} \int_{\Gamma(-H)} \partial_n E_z \, \overline{E_z} &= - \frac{\varepsilon_-}{\varepsilon_+ \kappa_-^2} \int_\Gamma \partial_n E_z \, \overline{E_z} \, , \\
\int_{\Omega_H \cap G_-} \frac{\mu_-}{\mu_+} \Big(\frac{1}{\kappa_-^2} |\nabla B_z|^2 - \omega^2 |B_z|^2 \Big) - \frac{\mu_-}{\mu_+ \kappa_-^2} \int_{\Gamma(-H)} \partial_n B_z \, \overline{B_z} &= - \frac{\mu_-}{\mu_+ \kappa_-^2} \int_\Gamma \partial_n B_z \, \overline{B_z} \, ,
\end{aligned}$$

such that the imaginary parts of Eqs. (24), (25) become

$$\begin{aligned}
- \operatorname{Im} \frac{\varepsilon_-}{\varepsilon_+ \kappa_-^2} \int_\Gamma \partial_n E_z \, \overline{E_z} + \sin\phi \operatorname{Im} \Big(\frac{1}{\kappa_+^2} - \frac{1}{\kappa_-^2} \Big) \int_\Gamma \partial_t B_z \, \overline{E_z} \\
- \frac{\beta}{\kappa_+^2} \Big(|E_0^+|^2 - |p_z|^2 \Big) - \sum_{\beta_n^+ > 0} \frac{\beta_n^+}{\kappa_+^2} |E_n^+|^2 = 0 \, , \\
- \operatorname{Im} \frac{\mu_-}{\mu_+ \kappa_-^2} \int_\Gamma \partial_n B_z \, \overline{B_z} - \sin\phi \operatorname{Im} \Big(\frac{1}{\kappa_+^2} - \frac{1}{\kappa_-^2} \Big) \int_\Gamma \partial_t E_z \, \overline{B_z} \\
- \frac{\beta}{\kappa_+^2} \Big(|B_0^+|^2 - |q_z|^2 \Big) - \sum_{\beta_n^+ > 0} \frac{\beta_n^+}{\kappa_+^2} |B_n^+|^2 = 0 \, .
\end{aligned}$$

Hence

$$\begin{aligned}
|p_z|^2 + |q_z|^2 &= \sum_{\beta_n^+ > 0} \frac{\beta_n^+}{\beta} \big(|E_n^+|^2 + |B_n^+|^2 \big) + \operatorname{Im} \frac{\varepsilon_- \kappa_+^2}{\varepsilon_+ \kappa_-^2 \beta} \int_\Gamma \partial_n E_z \, \overline{E_z} + \operatorname{Im} \frac{\mu_- \kappa_+^2}{\mu_+ \kappa_-^2 \beta} \int_\Gamma \partial_n B_z \, \overline{B_z} \\
&\quad - \frac{\sin\phi}{\beta} \Big(\operatorname{Im} \Big(1 - \frac{\kappa_+^2}{\kappa_-^2} \Big) \int_\Gamma (\partial_t B_z \, \overline{E_z} - \partial_t E_z \, \overline{B_z}) \Big) \\
&= \sum_{\beta_n^+ > 0} \frac{\beta_n^+}{\beta} \big(|E_n^+|^2 + |B_n^+|^2 \big) + \frac{\kappa_+^2}{\beta} \operatorname{Im} \int_\Gamma \Big(\frac{\varepsilon_-}{\varepsilon_+ \kappa_-^2} \partial_n E_z \, \overline{E_z} + \frac{\mu_-}{\mu_+ \kappa_-^2} \partial_n B_z \, \overline{B_z} \Big) \\
&\quad + \frac{2 \kappa_+^2 \sin\phi}{\beta} \operatorname{Im} \frac{1}{\kappa_-^2} \operatorname{Re} \int_\Gamma E_z \, \partial_t \overline{B_z} \, .
\end{aligned}$$

Thus we derive the conservation of energy for absorbing gratings

$$|p_z|^2 + |q_z|^2 = R + A$$

with the absorption energy of conical diffraction

$$A = \frac{\kappa_+^2}{\beta} \operatorname{Im}\left(\frac{1}{\kappa_-^2}\Big(\frac{\varepsilon_-}{\varepsilon_+}\int_\Gamma \partial_n E_z\,\overline{E_z} + \frac{\mu_-}{\mu_+}\int_\Gamma \partial_n B_z\,\overline{B_z} + 2\sin\phi\,\operatorname{Re}\int_\Gamma E_z\,\partial_t\overline{B_z}\Big)\right). \tag{26}$$

In the case $\phi = 0$ formula (26) provides the expressions of the heat absorption energy for in-plane diffraction derived in [29].

3. Numerical implementation

We discuss briefly the numerical solution of the system (23). Let Γ be parametrized by (13). In the case of a smooth profile Σ a trigonometric collocation method is used, i.e. we approximate

$$\begin{aligned} w(\sigma(t))\,\mathrm{e}^{-i\alpha X(t)}\,|\sigma'(t)| &\approx w_N(t) = \sum_{k=-N}^{N} a_k\,\mathrm{e}^{2\pi i k t}, \\ \tau(\sigma(t))\,\mathrm{e}^{-i\alpha X(t)}\,|\sigma'(t)| &\approx \tau_N(t) = \sum_{k=-N}^{N} b_k\,\mathrm{e}^{2\pi i k t}, \end{aligned} \tag{27}$$

and the coefficients $\{a_k\}, \{b_k\}$ are such that the system (23) is satisfied at the $2N+1$ collocation points $t_k = k/(2N+1)$, $k = 0, \ldots, 2N$.

Similar to [16] the advantage of trigonometric methods is utilized that the integral operators $V_\alpha^\pm$, H_α^+ and J_α^- with singular kernels can be approximated properly. For example, using the parametrization $\sigma(t)$ the single layer potential operator of w can be approximated by

$$V_\alpha^\pm w(\sigma(t)) \approx -2\,\mathrm{e}^{i\alpha X(t)}\Big(\int_0^1 \log|2\sin\pi(t-s)|\,w_N(s)\,ds + \int_0^1 g_\alpha^\pm(t,s) w_N(s)\,ds\Big)$$

and the singular integral $J_\alpha^\pm w$ by

$$J_\alpha^\pm w(\sigma(t)) \approx \mathrm{e}^{i\alpha X(t)}\Big(\int_0^1 \cot\pi(t-s)\,w_N(s)\,ds + \int_0^1 j_\alpha^\pm(t,s) w_N(s)\,ds\Big),$$

where the functions $g_\alpha^\pm(t,s), j_\alpha^\pm(t,s)$ are continuous and periodic in t and s. The action of the integral operators with the kernels $\log|2\sin\pi(t-s)|$ and $\cot\pi(t-s)$ on trigonometric polynomials is given analytically. All other integrals have continuous kernels and they are approximated by the trapezoidal rule like in Nyström's method. So the discretization error depends only on the error made in computing the functions $g_\alpha^\pm(t,s), j_\alpha^\pm(t,s)$ and the continuous kernels of K_α^+ and L_α^-, i.e. in computing the fundamental solution and there derivatives. Here we use the exact Ewald method (cf. [22]) with a number of summation terms to ensure discretization errors of order N^{-3}. Finally the operator products $V_\alpha^+ L_\alpha^-$, $K_\alpha^+ V_\alpha^-$, $H_\alpha^+ V_\alpha^-$ or $V_\alpha^+ J_\alpha^-$ are approximated by the products of the corresponding discretization matrices. Note that instead of $H_\alpha^+ V_\alpha^-$ or $V_\alpha^+ J_\alpha^-$ one can also perform the discretization of $V_\alpha^+ \partial_t V_\alpha^-$, involving a numerical differentiation. Numerical tests and further investigations can show which one is preferable for given efficiency calculations.

For the solution of the discrete system we use a preconditioned GMRES method similar to that described in [22]. The number of iterations until a prescribed residual error is reached, depends of course on the refraction indices and the profile, but it is nearly independent of the number of unknowns. However, it should be noted that modern implementations of the LAPACK and BLAS software packages on multiprocessor machines make direct solving to a competitive alternative to iterative solution methods even for rather large systems.

If the profile curve has corners, then the convergence properties of methods with only trigonometric trial functions deteriorate due to singularities of the densities w and τ of the form $O(\rho^{-\delta})$, $0 < \delta < 1$, where ρ is the distance to the closest edge. In boundary element methods it is common to use piecewise polynomial trial functions on meshes graded towards corner points. But due to the complicated form of their kernels the quadrature of the integral operators acting on piecewise polynomials is very expensive. Therefore we use a modification of the trigonometric collocation scheme with a fixed number of piecewise polynomial trial functions. First we introduce meshes of collocation points, which contain the corners and are graded towards the corner points. This can be derived by changing the parametrization (13), for example, if $\sigma(t_j)$ is a corner point, then $\sigma'(t_j) = \sigma''(t_j) = 0$ implies grading towards the corner. Further, for each collocation point t_k there exists a Lagrangian trigonometric polynomial $p_k(t)$ of degree $2N + 1$ such that

$$p_k(t_j) = \delta_{kj}\,, \quad k, j = 0, \ldots, 2N\,,$$

δ_{kj} is Kronecker's delta. For each edge and a fixed number of collocation points t_k around it we replace the corresponding Lagrangian trigonometric polynomial $p_k(t)$ by a cubic spline $s_k(t)$ on the graded mesh with $s_k(t_j) = \delta_{kj}$. Thus we get a hybrid trigonometric-spline collocation method, which combines the efficient computation of the integrals for trigonometric polynomials with the good approximation properties of piecewise polynomials on graded meshes near edges. The values at the collocation point t_j of the integrals on the basis spline s_k are computed by a composite Gauss-quadrature with a quadrature mesh geometrically graded towards t_j and depending on the distance $|\sigma(t_k) - \sigma(t_j)|$. This leads to a fixed number of additional calculations of the fundamental solutions $\Psi_{\omega\kappa_\pm,\alpha}$ for each discretisation level compared with the pure trigonometric method, which is however compensated by a significantly higher accuracy.

4. Numerical results

The workability of the code developed has been confirmed by numerous tests usually employed in classical and conical diffraction cases, more specifically: the reciprocity theorem; stabilization of results under doubling of the number of collocation points and varying of the calculation accuracy of kernel functions; comparison with analytically amenable cases of plane interfaces; consideration of the inverse (non-physical) radiation condition; use of different variants of collocation point distribution on boundaries (mesh refinements); comparison with the results obtained by another of our codes or with published data, or with information corresponded to us by other researchers, including results of measurements. A small part of such numerical tests is demonstrated in this Section.

4.1. **Comparing.** In Table 1 the numerical results of the present boundary integral equation method (IM) for a dielectric lamellar grating with the ridge c in a conical mounting are compared with those of Table 2 of Li who uses the modal method (MM) [33]. All grating and light parameters are listed in the table caption. The agreement between the MM and the IM for the efficiencies and polarization angles is almost perfect for all reflection and transmission orders despite of very different methods compared. Note that we use the same definitions for polarization angles as in Refs. [30, 33]. We used 400 collocation points, mesh grading, and the direct discretization of J_α^- to calculate this example that allocates 188 MByte memory. The energy balance error calculated from (26) is about 10^{-5}. The average time taken up by the example on a portable workstation IBM ThinkPad® R50p with an Intel® Pentium® M 1.7 GHz processor and 2 GByte of RAM is about 4 sec when operating on Linux (kernel 2.6.17).

In Table 2 the numerical results of a similar comparison as in Table 1 between the IM and the MM are demonstrated for a conducting lamellar grating in a conical mounting (compare with Table 3 of [33]). All grating and light parameters are listed in the table caption. The agreement between the MM and the IM for the efficiencies and polarization angles is, in general, good. The same accuracy parameters as in the previous example have been used and similar calculation times have been obtained on the above mentioned laptop. The energy balance error calculated from (26) is about 10^{-6}.

In Tables 3 and 4 the numerical results of the IM for a dielectric sine grating in a conical mounting are compared with those of Table 2 of Ref. [7] of Li who used for the presented data the coordinate transformation method (CM) [5]. All grating and light parameters are listed in the table captions. The agreement between the CM and the IM for the efficiencies is very good. We used 100 collocation points and the numerical differentiation of V_α^+ to calculate this example that allocates 10 MByte of RAM. The energy balance error calculated from (26) is about 10^{-5} for both components of the incident radiation. The average computation time taken up by the example on the above mentioned laptop is about 0.2 sec.

The results of another comparison for a metal echelette grating with the blaze angle ζ in a conical mounting are demonstrated in Tables 5 and 6 compared with those [34] updated by Li who has used again the CM to calculate the efficiency of the grating having edges [35]. All grating and light parameters are listed in the table captions. As one can see in Tables 5 and 6, again the agreement between the CM and the IM is very good for the all order efficiencies and polarization angles. One has used 800 collocation points, mesh scaling near edges, and the differentiation of V_α^+ to calculate this example allocating 196 MByte of RAM. The average energy balance error calculated from Eq. (26) is about 10^{-5} for both polarization states of the incident radiation. The average computation time taken up by two values of the polarization angle on the above mentioned laptop is about 18 sec.

4.2. **Convergence, accuracy, and computation time.** We will examine the convergence rate and the accuracy of diffraction efficiencies with respect to the number of collocation points N. For the efficiency convergence testing, a magnitude of computational error cannot be reliably deduced from accuracy criteria based on a single computation such as the energy balance and the inverse radiation condition tests. For this purpose comparative studies should be used, i.e. N-doubling or changing the configuration of collocation points. We introduce a parameter $\Delta_{N,k}$ as an integral measure of the efficiency error under N-doubling tests. It is equal to the sum of absolute differences of respective diffraction order efficiencies for two successive iterations with the number of collocation points for each iteration of $N = N_0 \times 2^{k-1}$, where N_0 is the initial number of collocation points, $k = 1, ..., K$, and K is the total number of iterations. The magnitude of $\Delta_{N,k}$ gives approximately the correct digits in the numerical results if the number of propagating diffraction orders is small enough or only a few valuable orders exist. For many propagating orders it can give a more pessimistic error value.

To examine the convergence of diffraction efficiencies, we choose as a sample the slanted lamellar highly-conducting grating similar to that from Figs. 10 and 11 of Ref. [36], but for $\varepsilon_- = (-10^4, 0)$ That means that we study almost perfectly conducting non-function-profiled grating with the zero real part of the refractive index and its imaginary part of 10^2 using our solver for the finite conductivity, the case probably not possible for many rigorous methods, even with all known improvements and artificial inclusions [36]. Note that using the refractive index of $(10^{-2}, 10)$ from the example of Ref. [36] the convergence rate of our solver is so fast that no interesting data to discuss can be seen even for small values of N. So in Fig.

2 the convergence of the diffraction efficiencies with respect to the truncation parameter N under N-doubling is demonstrated for $N_0 = 15$ and $K = 9$ using the much harder refractive index mentioned above. The efficiency values stabilize and the convergence is starting at $N = 60$ and achieved with the high accuracy at $N = 960$. Note that $\Delta_{1920,8} = 4.21 \times 10^{-4}$ and $\Delta_{3840,9} = 1.50 \times 10^{-4}$ and the energy balance error is about 10^{-4} for these values of N.

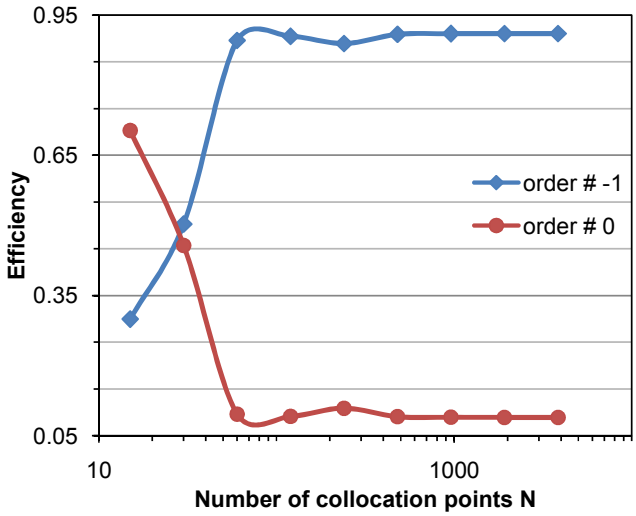

FIGURE 2. Diffraction efficiencies of a lamellar highly-conducting grating with $c/d = 0.5$ and $2H/d = 0.3$ having the grooves slanted at angle of 45° vs. number of collocation points N. Other parameters: $\epsilon_+ = 1$, $\epsilon_- = (-10^4, 0)$, $\mu_\pm = 1$, $\lambda/d = 0.8$, $\theta^i = 26.565°$, $\phi^i = 14.478°$, $\delta^i = 0$, and $\psi^i = 0$.

Thus, the convergence rate is fast enough taking into account the difficult case tested. Moreover, due to solution peculiarities for profiles with edges the convergence rate even is better for $\varepsilon_- = (-10^5, 0)$, but the calculation time is longer. The absorption calculated from Eq. (26) is very small for a such grating ($\sim 10^{-5}$) and its non-negative magnitude and decreasing are also a good measure of the convergence and the calculation accuracy. One can also check of the absolute accuracy of calculation results for this example using the perfect conductivity approximation. The asymptotic efficiency values calculated using this approximation differ from those obtained using the finite conductivity approach (0.9105 and 0.0894 for -1 and 0 orders, respectively) by not more than a few hundredths of a %. The total computation time of all results presented in Fig. 3 is about 35 minutes on the above mentioned PC and the required RAM is about 2 GB. Non-using a mesh refinement and using the differentiation of V_α^+ are most suitable for this sort of calculations.

The computation time T for the considered one-border conical diffraction solver is essentially a function of the truncation parameter N only. The general dependence $T(N)$ of boundary integral equation formalisms is proportional to N^3 due to a square dependence on N for the Green functions and their derivatives calculations and the summation of these computed values that is proportional to N [15, 16, 17]. In addition, a direct linear equation solver requires a time that is also proportional to N^3. To speed-up the presented calculation solver two substantial accelerations have been used. The first one is the Ewald's method for the kernel computation; the second one is solving systems of linear equations iteratively. As a result, the computation time is proportional to N^2 that clearly seen in Fig. 3 for the typical example described in Table 2. If the iterative solver cannot give correct results after the given number of iterations, then the direct solver is applied. Fortunately, this situation occurs in infrequent or hard cases only.

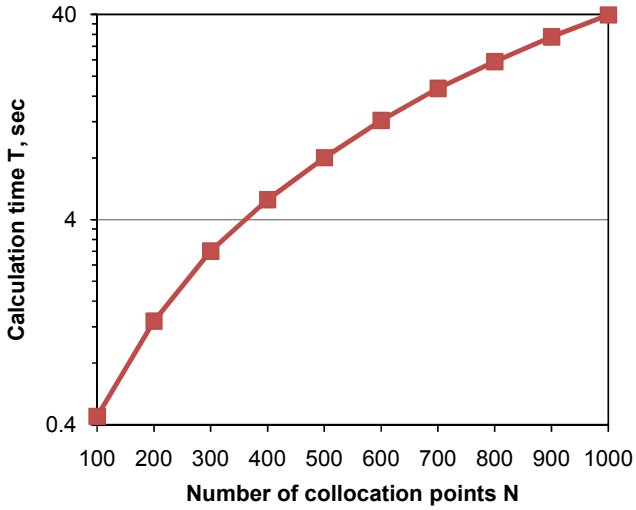

FIGURE 3. The computation time for the example described in Table 2.

4.3. **Efficiency of a grazing-incidence real-groove-profile off-plane grating in x-rays.** Grazing-incidence off-plane gratings have been suggested for the International X-ray Observatory (IXO) [37]. Compared with gratings in the classical in-plane mount, x-ray gratings in the off-plane mount have the potential for superior resolution and efficiency for the IXO mission. The results of efficiency calculations for such a gold blazed soft x-ray grating in a conical mount using the groove profile derived from Atomic Force Microscopy (AFM) measurements are shown in Fig. 4. The average border shape having 123 nodes is presented in Fig. 5. All grating and light parameters are listed in the figure caption. The incident beam in the rigorous calculations was assumed to be 81% TM-polarized that means the electric vectors of the incident wave and the diffracted waves are approximately parallel to the surface of the grating at the given diffraction angles. In Fig. 5 the numerical results of the presented BIEM for a finite boundary conductivity are compared with those based on the BIEM with the perfect conductivity approximation. The incident beam in the computations based on the perfect conductivity approximation was assumed to be 100% TE-polarized.

Rigorous computations carried out by the presented method show that for the considered grating model all the order efficiencies are not sensitive to a polarization state and efficiency jumps do not occur in the wavelength range investigated. For any polarization state order efficiencies differ from those presented in Fig. 4 not more than a few tenths of a %. Contrary, calculations based on the perfectly conducting boundary approximation are very sensitive to the polarization state and sharp Rayleigh anomalies for the TM-polarized incident radiation occur. They were predicted earlier for such a grating using the in-plane boundary integral equation method and the Invariance theorem [39]. As it can be seen in Fig. 4, the agreement between rigorously calculated data and those obtained by the perfect conductivity approximation multiplied by Fresnel reflectances is good only if the TE-polarized incident radiation is used for the approximation.

It has been used 800 collocation points, no mesh scaling, and the differentiation of V_α^+ to calculate rigorously this real groove profile example that allocates a space of 144 MByte. The energy balance error calculated from Eq. (26) is about 10^{-4} in the investigated wavelength range. The average computation time taken up by one wavelength on the above mentioned laptop is about 40 sec. The time of an approximate computation is about five times shorter for the same accuracy.

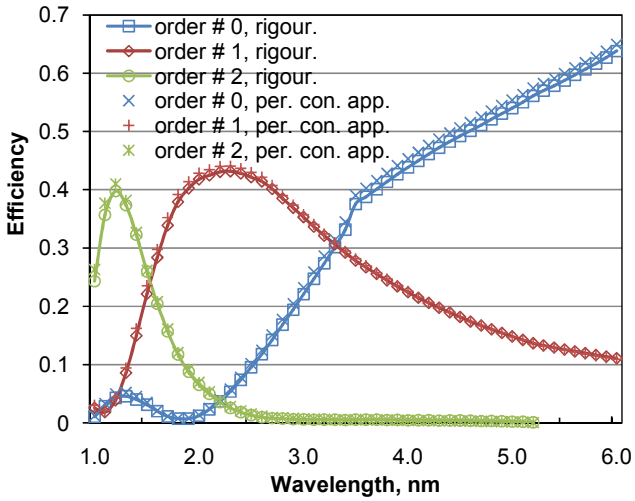

FIGURE 4. Diffraction efficiencies of a gold polygonal grating with 123 nodes, $\mu_\pm = 1$ and $d = 200$ nm for the incident wave with $\theta^i = -30°$ and $\phi^i = 88°$: rigorously ($\delta^i = 34.143°$ and $\psi^i = 0$) or using the perfect conductivity approximation ($B_z \approx 0$: $\delta^i = 30.015°$ and $\psi^i = 180°$) vs. wavelength λ. Refractive indices of Au were taken from Ref. [38]

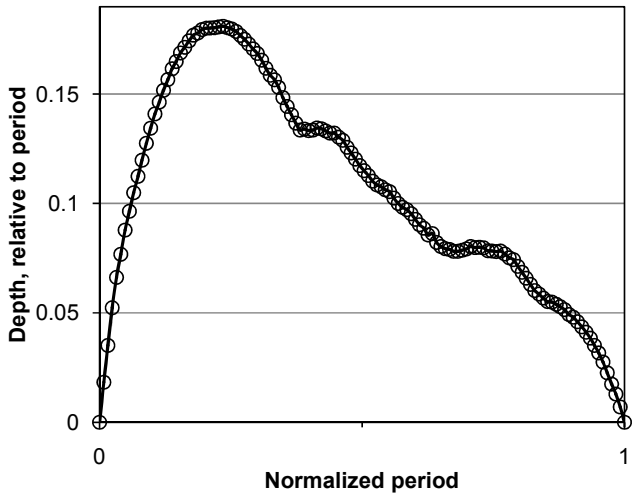

FIGURE 5. AFM-measured average groove profile.

5. SUMMARY AND CONCLUSIONS

Off-plane scattering of time-harmonic plane waves by 1D structures has been considered. The term '1D' refers to a general diffraction grating or a rough mirror having arbitrary conductivity on a planar surface in $\mathbb{R}^3$, which is periodic in one surface direction, constant in the second, and has an arbitrary border profile including edges and non-functions. The electromagnetic formulation of conical diffraction by gratings reduced to a system of 2 Helmholtz equations in $\mathbb{R}^2$, which are coupled by transmission conditions at the interfaces between different materials, was presented.

The integral equations for conical diffraction were obtained using the boundary integrals of the single and double layer potentials including the tangential derivative of single layer potentials interpreted as singular integrals. A full rigorous theoretical foundation of the conical boundary integral equation method was established for the first time. Besides, we

derived an important formula for direct calculation of the absorption of gratings in conical diffraction mounts. Some rules which are expedient for the numerical implementation of the described theory were presented.

The results of efficiencies and polarization angles comparing with the data obtained by Li using the modal (lamellar profiles) and the coordinate transformation (sinus and echelette profiles) conical solvers for transmission and reflection gratings are in a good agreement. The high rate of convergence, the high accuracy, and the short computation time of the presented solver were demonstrated for various samples. An example of rigorous efficiency computations of the soft x-ray grazing-incidence off-plane grating suggested for the IXO mission was demonstrated using the 123-node AFM-measured border profile and realistic refractive indices data.

The solver developed and tested is found to be accurate and efficient for solving conical diffraction problems including difficult cases of high-conductive surfaces, borders with edges, real border profiles, and gratings working at very short wavelengths.

TABLE 1. Diffraction Angles (θ, ϕ), Diffraction Efficiencies (η), and Polarization Angles (δ, ψ) of a Dielectric Lamellar Grating[a]

DO[b]	θ(IM),°	ϕ(IM),°	η(MM),%	η(IM),%	δ(MM),°	δ(IM),°	ψ(MM),°	ψ(IM),°
R_{-2}	35.265	−30	0.1614	0.1612	64.32	64.32	−30.30	−30.24
R_{-1}	0	−30	0.3807	0.3807	65.97	66.0	−157.20	−157.22
R_0	35.264	−30	1.855	1.854	70.49	70.43	−148.46	−148.60
T_{-3}	−45	−19.471	3.363	3.363	51.06	51.05	32.28	32.28
T_{-2}	−20.705	−19.471	10.34	10.35	56.24	56.24	110.21	110.23
T_{-1}	0	−19.471	31.87	31.87	46.55	46.54	99.03	99.02
T_0	20.705	−19.471	14.19	14.19	34.26	34.26	68.37	68.38
T_1	45	−19.471	37.83	37.83	46.33	46.34	86.81	86.83

[a] $c/d = 0.5$, $2H/d = 0.5$, $\epsilon_+ = 1$, $\epsilon_- = 2.25$, $\mu_\pm = 1$, $\lambda/d = 0.5$, $\theta^i = 35.264°$, $\phi^i = 30°$, $\delta^i = 45°$, and $\psi^i = 90°$. IM stands for the present integral method, MM stands for the Li's modal method.
[b] Diffraction order.

TABLE 2. Diffraction Angles (θ, ϕ), Diffraction Efficiencies (η), and Polarization Angles (δ, ψ) of a Metallic Lamellar Grating[a]

DO[b]	θ(IM),°	ϕ(IM),°	η(MM),%	η(IM),%	δ(MM),°	δ(IM),°	ψ(MM),°	ψ(IM),°
R_{-2}	−43.715	−20.705	7.31	7.52	62.48	61.85	52.74	48.30
R_{-1}	−9.007	−20.705	13.51	13.25	15.35	15.79	−12.05	−12.23
R_0	22.208	−20.705	42.99	44.27	41.25	41.33	171.21	170.15
R_1	65.852	−20.705	30.24	31.05	75.23	75.64	168.78	166.30

[a] $c/d = 0.5$, $2H/d = 1$, $\epsilon_+ = 1$, $\epsilon_- = (-24.99, 1)$, $\mu_\pm = 1$, $\lambda/d = 0.5$, $\theta^i = 22.208°$, $\phi^i = 20.705°$, $\delta^i = 45°$, and $\psi^i = 0$. IM stands for the present integral method, MM stands for the Li's modal method.
[b] Diffraction order.

TABLE 3. Diffraction Angles (θ, ϕ), Diffraction Efficiencies (η), and Polarization Angles (δ, ψ) of a Dielectric Sine Grating for $B_z = 0^a$

DO[b]	θ(IM),°	ϕ(IM),°	η(CM),%	η(IM),%	δ(CM),°	δ(IM),°	ψ(CM),°	ψ(IM),°
R_{-3}	−43.384	−15	1.121	1.121	71.01	70.99	3.62	3.60
R_{-2}	−9.744	−15	3.741	3.741	26.91	26.90	0.93	0.93
R_{-1}	20.389	−15	3.873	3.873	63.25	63.25	178.16	178.18
R_0	60	−15	10.33	10.33	88.93	88.93	178.06	178.05
T_{-5}	−57.013	−7.435	.01858	.01855	80.18	80.19	−114.16	−114.68
T_{-4}	−35.921	−7.435	.002466	.002482	52.39	52.58	99.81	100.24
T_{-3}	−19.545	−7.435	.7396	.7394	57.62	57.61	−179.23	−179.28
T_{-2}	−4.729	−7.435	4.922	4.922	22.89	22.90	174.83	174.84
T_{-1}	9.770	−7.435	9.925	9.923	60.39	60.39	4.71	4.72
T_0	24.949	−7.435	7.146	7.145	77.33	77.32	6.83	6.84
T_1	42.371	−7.435	51.83	51.83	84.43	84.43	−5.77	−5.78
T_2	67.826	−7.435	6.351	6.351	84.85	84.85	−11.33	−11.39

[a] $2H/d = 0.3$, $\epsilon_+ = 1$, $\epsilon_- = 4$, $\mu_\pm = 1$, $\lambda/d = 0.5$, $\theta^i = 60°$, $\phi^i = 15°$, $\delta^i = 81.501°$, and $\psi^i = 0$. IM stands for the present integral method, CM stands for the Li's coordinate transformation method.
[b]Diffraction order.

TABLE 4. Diffraction Angles (θ, ϕ), Diffraction Efficiencies (η), and Polarization Angles (δ, ψ) of a Dielectric Sine Grating for $E_z = 0^a$

DO[b]	θ(IM),°	ϕ(IM),°	η(CM),%	η(IM),%	δ(CM),°	δ(IM),°	ψ(CM),°	ψ(IM),°
R_{-3}	−43.384	−15	1.121	1.121	71.01	70.99	3.62	3.60
R_{-2}	−9.744	−15	3.741	3.741	26.91	26.90	0.93	0.93
R_{-1}	20.389	−15	3.873	3.873	63.25	63.25	178.16	178.18
R_0	60	−15	10.33	10.33	88.93	88.93	178.06	178.05
T_{-5}	−57.013	−7.435	.01858	.01855	80.18	80.19	−114.16	−114.68
T_{-4}	−35.921	−7.435	.002466	.002482	52.39	52.58	99.81	100.24
T_{-3}	−19.545	−7.435	.7396	.7394	57.62	57.61	−179.23	−179.28
T_{-2}	−4.729	−7.435	4.922	4.922	22.89	22.90	174.83	174.84
T_{-1}	9.770	−7.435	9.925	9.923	60.39	60.39	4.71	4.72
T_0	24.949	−7.435	7.146	7.145	77.33	77.32	6.83	6.84
T_1	42.371	−7.435	51.83	51.83	84.43	84.43	−5.77	−5.78
T_2	67.826	−7.435	6.351	6.351	84.85	84.85	−11.33	−11.39

[a] $2H/d = 0.3$, $\epsilon_+ = 1$, $\epsilon_- = 4$, $\mu_\pm = 1$, $\lambda/d = 0.5$, $\theta^i = 60°$, $\phi^i = 15°$, $\delta^i = 8.499°$, and $\psi^i = 180°$. IM stands for the present integral method, CM stands for the Li's coordinate transformation method.
[b]Diffraction order.

TABLE 5. Diffraction Angles (θ, ϕ), Diffraction Efficiencies (η), and Polarization Angles (δ, ψ) of a Metallic Echelette Grating for $\delta^i = 0^a$

DO[b]	θ(IM),°	ϕ(IM),°	η(CM),%	η(IM),%	δ(CM),°	δ(IM),°	ψ(CM),°	ψ(IM),°
R_{-1}	-40.746	-40	12.99	12.97	39.409	39.447	-175.87	-175.93
R_0	0	-40	28.49	28.45	86.449	86.414	-51.16	-50.97
R_1	40.746	-40	24.77	24.81	39.237	39.209	7.58	7.67

[a] $\zeta = 30°$, $\epsilon_+ = 1$, $\epsilon_- = (-45, 28)$, $\mu_\pm = 1$, $\lambda/d = 0.5$, $\theta^i = 0$, $\phi^i = 40°$, and $\psi^i = 0$. IM stands for the present integral method, CM stands for the Li's coordinate transformation method.
[b] Diffraction order.

TABLE 6. Diffraction Angles (θ, ϕ), Diffraction Efficiencies (η), and Polarization Angles (δ, ψ) of a Metallic Echelette Grating for $\delta^i = 90°^a$

DO[b]	θ(IM),°	ϕ(IM),°	η(CM),%	η(IM),%	δ(CM),°	δ(IM),°	ψ(CM),°	ψ(IM),°
R_{-1}	-40.746	-40	53.15	53.15	54.0	54.0	13.31	13.37
R_0	0	-40	17.51	17.48	4.53	4.58	95.49	95.21
R_1	40.746	-40	9.423	9.444	49.47	49.41	-171.24	-171.22

[a] $\zeta = 30°$, $\epsilon_+ = 1$, $\epsilon_- = (-45, 28)$, $\mu_\pm = 1$, $\lambda/d = 0.5$, $\theta^i = 0$, $\phi^i = 40°$, and $\psi^i = 0$. IM stands for the present integral method, CM stands for the Li's coordinate transformation method.
[b] Diffraction order.

ACKNOWLEDGEMENTS

The authors feels indebted to Lifeng Li (Tsinghua University, China) for the information provided and fruitful testing. Helpful discussions with Bernd Kleemann (Carl Zeiss AG, Germany), Andreas Rathsfeld (WIAS, Germany), and Sergey Sadov (New Foundland Memorial University, Canada) are greatly appreciated.

REFERENCES

[1] P. Vincent, "Differential Methods," in *Electromagnetic theory of gratings. Topics in Current Physics, Vol. 22*, R. Petit, ed. (Springer, 1980), pp. 101–121.
[2] M. Neviere and E. Popov, *Light Propagation in Periodic Media: Differential Theory and Design* (Marcel Dekker, 2002).
[3] E. Popov and L. Mashev, "Conical diffraction mounting generalization of a rigorous differential method," J. Optics, **17**, pp. 175–180 (1986).
[4] S.J. Elston, G.P. Bryan-Brown, and J.R. Sambles, "Polarization conversion from diffraction gratings," Phys. Rev. B **44**, pp. 6393–6400 (1991).
[5] L. Li, "Multilayer coated diffraction gratings: Differential method of Chandezon et al. revisited," J. Opt. Soc. Am. A **11**, pp. 2816–2828 (1994).
[6] J.P. Plumey, G. Granet, and J. Chandezon, "Differential covariant formalizm for solving Maxwell's equations in curvilinear coordinates: oblique scattering from lossy periodic surfaces," IEEE Trans. Antennas Propag. **43**, pp. 835–842 (1995).
[7] L. Li, "Multilayer modal method for diffraction gratings of arbitrary profile, depth, and permittivity," J. Opt. Soc. Am. A **10**, pp. 2581–2591 (1993).
[8] F. Zolla and R. Petit, "Method of fictitious sources as applied to the electromagnetic diffraction of a plane wave by a grating in conical diffraction mounts," J. Opt. Soc. Am. A **13**, pp. 796–802 (1996).
[9] Ch. Hafner, *Post-modern Electromagnetics: Using Intelligent Maxwell Solvers* (Wiley, 1999).

[10] J. Elschner, R. Hinder, and G. Schmidt, "Finite element solution of conical diffraction problems," Adv. Comp. Math. **16**, pp. 139–156, (2002).
[11] R. Köhle, "Rigorous simulation study of mask gratings at conical illumination," Proc. SPIE **6607**, 66072Z-1–10 (2007).
[12] L. Tsang, J.A. Kong, K.-H. Ding, and C.O. Ao, "Scattering and emission by a periodic rough surface," in *Scattering of Electromagnetics Waves: Numerical Simulations*, (Wiley, 2001), pp. 61–110.
[13] D.W. Prather, M.S. Mirotznik, and J.N. Mait, "Boundary integral methods applied to the analysis of diffractive optical elements," J. Opt. Soc. Am. A **14**, pp. 34–43 (1997).
[14] J.M. Bendickson, E.N. Glytsis, and T.K. Gaylord, "Modeling considerations for rigorous boundary element method analysis of diffractive optical elements," J. Opt. Soc. Am. A **18**, pp. 1495–1507 (2001).
[15] E.G. Loewen and E. Popov, "Review of Electromagnetic Theories of Grating Efficiencies," in *Diffraction Gratings and Applications, Optical Engineering Series* (Marcel Dekker, 1997), pp. 367–399.
[16] D. Maystre, M. Neviere, and R. Petit, "Experimental verifications and applications of the theory", in *Electromagnetic theory of gratings. Topics in Current Physics, Vol. 22*, R. Petit, ed. (Springer, 1980), pp. 159–225.
[17] L.I. Goray, I.G. Kuznetsov, S.Yu. Sadov, and D.A. Content, "Multilayer resonant subwavelength gratings: effects of waveguide modes and real groove profiles," J. Opt. Soc. Am. A **23**, pp. 155–165 (2006).
[18] B.H. Kleemann and J. Erxmeyer, "Independent electromagnetic optimization of the two coating thicknesses of a dielectric layer on the facets of an echelle grating in Littrow mount," J. Mod. Opt. **51**, pp. 2093–2110 (2004).
[19] M. Saillard and D. Maystre, "Scattering from metallic and dielectric surfaces," J. Opt. Soc. Am. A **7**, pp. 982–990 (1990).
[20] B.H. Kleemann, J. Gatzke, Ch. Jung, and B. Nelles, "Design and efficiency characterization of diffraction gratings for applications in synchrotron monochromators by electromagnetic methods and its comparison with measurement," Proc. SPIE **3150**, pp. 137–147 (1997).
[21] L.I. Goray and J.F. Seely, "Efficiencies of master replica, and multilayer gratings for the soft-x-ray-extreme-ultraviolet range: modeling based on the modified integral method and comparisons with measurements," Appl. Opt. **41**, pp. 1434–1445 (2002).
[22] A. Rathsfeld, G. Schmidt, and B.H. Kleemann, "On a fast integral equation method for diffraction gratings," Comm. Comp. Phys. **1**, pp. 984–1009 (2006).
[23] D. Maystre, "Integral Methods," in *Electromagnetic theory of gratings. Topics in Current Physics, Vol. 22*, R. Petit, ed. (Springer, 1980), pp. 53–100.
[24] A. Pomp, "The integral method for coated gratings: computational cost," J. Mod. Opt. **38**, pp. 109–120 (1991).
[25] B. Kleemann, A. Mitreiter, and F. Wyrowski, "Integral equation method with parametrization of grating profile. Theory and experiments," J. Mod. Opt. **43**, pp. 1323–1349 (1996).
[26] E. Popov, B. Bozhkov, D. Maystre, and J. Hoose, "Integral method for echelles covered with lossless or absorbing thin dielectric layers," Appl. Opt. **38**, pp. 47–55 (1999).
[27] L.I. Goray, "Modified integral method for weak convergence problems of light scattering on relief grating," Proc. SPIE **4291**, pp. 1–12 (2001).
[28] L.I. Goray and S.Yu. Sadov, "Numerical modeling of coated gratings in sensitive cases," in *Diffractive Optics and Micro-Optics*, R. Magnusson, ed., Vol. 75 of OSA Trends in Optics and Photonics Series (Optical Society of America, 2002), pp. 366–379.
[29] L.I. Goray, J.F. Seely, and S.Yu. Sadov, "Spectral separation of the efficiencies of the inside and outside orders of soft-x-ray-extreme ultraviolet gratings at near normal incidence," J. Appl. Phys. **100**, 094901-1–13 (2006).
[30] L.I. Goray, "Specular and diffuse scattering from random asperities of any profile using the rigorous method for x-rays and neutrons," Proc. SPIE **7390-30**, 73900V-1–11 (2009).
[31] J. Elschner, R. Hinder, F. Penzel, and G. Schmidt, "Existence, uniqueness and regularity for solutions of the conical diffraction problem," Math. Mod. Meth. Appl. Sci. **10**, pp. 317–341 (2000).
[32] G. Schmidt, "Boundary Integral Methods for Periodic Scattering Problems," in *Around the Research of Vladimir Maz'ya II. Partial Differential Equations*, (Springer, 2010), pp. 337–364.
[33] L. Li, "A modal analysis of lamellar diffraction gratings in conical mountings," Jour. of Modern Opt. **40**, pp. 553–573 (1993).
[34] M. Mansuripur, L. Li, and W.-H. Yeh, "Diffraction Gratings: Part 2," Optics and Photonic News, August (1999), pp. 44–48.
[35] L. Li and J. Chandezon, "Improvement of the coordinate transformation method for surface-relief gratings with sharp edges," J. Opt. Soc. Am. A **13**, pp. 2247–2255 (1996).

[36] E. Popov, B. Chernov, M. Neviere, and N. Bonod, "Differential theory: application to highly conducting gratings," J. Opt. Soc. Am. A **21**, pp. 199–206 (2004).
[37] http://ixo.gsfc.nasa.gov/technology/xgs.html.
[38] http://henke.lbl.gov/optical_constants/.
[39] J.F. Seely, L.I. Goray, B. Kjornrattanawanich, J.M. Laming, G.E. Holland, K.A. Flanagan, R.K. Heilmann, C.-H. Chang, M.L. Schattenburg, and A.P. Rasmussen, "Efficiency of a grazing-incidence off-plane grating in the soft-x-ray region," Appl. Opt. **45**, pp. 1680–1687 (2006).